J Appl Electrochem (2013) 43:375–385
DOI 10.1007/s10800-012-0522-1

ORIGINAL PAPER

Electrochemical lithiation and compatibility of graphite anode using glutaronitrile/dimethyl carbonate mixtures containing LiTFSI as electrolyte

Mouad Dahbi · Fouad Ghamouss · Mérièm Anouti · Daniel Lemordant · François Tran-Van

Received: 22 October 2012 / Accepted: 27 December 2012 / Published online: 10 January 2013

Abstract The compatibility of glutaronitrile (GLN) and its mixtures with dimethyl carbonate (DMC) containing lithium bis-(trifluoromethane sulfonyl) imide (LiTFSI) with graphite negative electrode was investigated. GLN/DMC/LiTFSI electrolytes' mixtures were characterized in terms of their ionic conductivities and viscosities. Cyclic voltammetry, galvanostatic charge–discharge, and electrochemical impedance spectroscopy were performed in order to study the performances of the graphite anode in the GLN-based electrolytes. Results clearly indicate that no significant Li intercalation occurs in graphite in pure GLN, but when GLN/DMC (1:1 and 1:3 w/w) mixtures were used, the cycling ability of the electrode was improved as the coulombic efficiency reaches 98 and 99 %, respectively. Moreover, SEM images of the graphite anode indicate that after being cycled in GLN-based electrolytes, the electrode surface was homogenously covered by a Solid Layer Interface which insures a reversible lithiation of graphite anode.

Keywords Electrolyte · Glutaronitrile · Lithium intercalation · Graphite anode · Solid Electrolyte Interface (SEI)

1 Introduction

Lithium ion batteries are widely used in large- and small-scale electronics devices due to their high gravimetric energy and power density compared to other batteries. In such devices, negative electrodes are typically based on lithium intercalation compounds having for the best of them a potential close to 0 V versus Li/Li^+. Among all anodic active materials, lithium intercalated graphite is by far the most used in lithium ion batteries [1–3]. Nowadays, processes occurring in lithium ion batteries are well known, and lithium intercalation into graphite and the formation of the Solid Electrolyte Interface layer (SEI) are undoubtedly the key phenomena occurring in such systems [4–6]. Lithium battery electrolytes typically consist of a binary or ternary mixture of alkyl carbonates containing a lithium salt such as $LiPF_6$. Challenging salts have also been proposed and among them we may cite lithium bis-oxalatoborate (LiBOB), lithium bis-(trifluoromethane sulfonyl) imide (LiTFSI), lithium bis-(pentafluoroethyl sulfonyl) amidure (LiBETI), lithium fluoroalkylphosphate (LiFAP), and Lithium bis-(fluorosulfonyl) imide (LiFSI) [7–11]. Most used alkyl carbonates are cyclic carbonates, ethylene carbonate (EC) and propylene carbonate (PC), and acyclic alkyl carbonates, dimethyl carbonate (DMC), ethyl methyl carbonate (EMC), and diethyl carbonate (DEC). Cyclic carbonates are highly polar, so more suitable for Li salts' dissolution and dissociation at high concentrations (1 M or more). As cyclic alkyl carbonates are rather viscous or solid at ambient temperature (EC melting temperature is 39 °C), more fluid acyclic alkyl carbonates are added in order to decrease the viscosity and thus increase the conductivity. To improve the stability of the SEI layer, and subsequently the electrode cyclability, some additives, such as fluoroethylene carbonate (FEC), chloroethylene carbonate (ClEC), or vinylene carbonate (VC), are added to the electrolytes [12, 14]. Despite the growing importance of lithium ion batteries, fundamental studies on the graphite negative electrode are insufficient; a complete understanding of all phenomena occurring at the graphite/electrolyte interface and the

M. Dahbi · F. Ghamouss (✉) · M. Anouti · D. Lemordant · F. Tran-Van
Laboratoire de Physico-Chimie des Matériaux et des Electrolytes pour L'Energie (PCM2E), Université François Rabelais EA 6299, Parc de Grandmont, 37200 Tours, France
e-mail: fouad.ghamouss@univ-tours.fr

compatibility of the electrode with different solvents and lithium salts is not reached. As an example, dimethoxyethane (DME) and dimethylsulfoxide (DMSO) tend to be co-intercalated into graphite, thus inhibiting the reversible intercalation–deintercalation of lithium. On the other hand, in binary electrolyte systems, DMSO/DMC and DME/DMC, the solvent co-intercalation has been drastically reduced [18]. Propylene carbonate which possesses a moderate viscosity and a high dielectric constant, and therefore suitable physicochemical properties for electrolyte, causes exfoliation of graphite and cannot be used in Li-ion system without SEI builder additives (EC, VC). Alternative solvents have been proposed to overcome issues related to the high melting point of EC and its relatively low oxidation potentials [15–19]. Recently, and on the basis of the earlier works of Ue et al. [19, 20] on the possible use of dinitrile solvents for high voltage storage devices, Y. Abu-Lebdeh et al. [15, 16] highlighted a large electrochemical window and especially a high resistivity toward oxidation (up to 6 V vs. Li/Li^+) of electrolytes containing dinitriles such as GLN (Glutaronitrile) or ADN (Adiponitrile). Moreover, the authors showed an improvement of the resistance of the Aluminum current collector to electrochemical corrosion even with LiTFSI salt which is known to lead to depassivation of Al and its oxidation. This latter result indicates that LiTFSI, which is chemically and thermally more stable than $LiPF_6$, could be used as an alternative lithium salt in Li-ion systems. LiTFSI- and $LiPF_6$-based electrolytes exhibit nearly the same performances (specific capacity on activated carbon and graphite, conductivity…) as we showed in a recent paper [25]. Even if it is more expensive than conventional salts such as $LiPF_6$, LiTFSI shows some interesting properties. For example, LiTFSI is more soluble than $LiPF_6$ in aprotic solvents and the binding energy between $TFSI^-$ and Li^+ is relatively low owing to the large anion size and its delocalized charge leading to an enhanced Li^+ transport [31]. As an example, in glutraonitrile, LiTFSI is soluble to more than 1 M and not $LiPF_6$. In addition, in references [15, 16], a fair cycling performance using a $MCMB/LiCoO_2$ battery has been reported using LiTFSI salt in EC/GLN mixture. EC was used as co-solvent and SEI builder. More recently, Nagahama et al. [17] examined the compatibility and the cathodic behavior of a series of six dinitrile-based solvents including GLN, ADN, and other dinitriles with different chain lengths. Otherwise, the authors showed that conventional cathode used in lithium ion batteries such as $LiFePO_4$ could be charged up to 6 V in a sebaconitrile-based electrolyte without any electrochemical decomposition. In the same work, the authors demonstrated that very recently, Gmitter et al. [21] reported good cycling performances in Methoxypropionitrile (MCN) and ADN of graphite anode when they used cyclic carbonate additives (FEC) as SEI builder and stabilizer. In all these works, authors used cyclic carbonate (EC or FEC) to build a stable and conductive SEI layer on the graphite electrode, but the compatibility of graphite directly exposed and cycled in dinitrile-based electrolyte without the SEI additives (FEC, VC, or EC) is still debated. We believe that such a question is crucial for the better understanding of processes occurring in Li-ion systems and the role of such components of electrolyte mixture.

This paper deals with the possible use of GLN as a solvent in single or binary electrolyte and its compatibility with graphite negative electrode. GLN-based electrolytes were used without any SEI additive and DMC was chosen as a co-solvent to decrease the viscosity of GLN and hence increase the conductivity of the electrolyte. The performances of the graphite electrode are discussed on the basis of galvanostatic charge–discharge cycling and impedance measurements. Additionally, scanning electron microscopy (SEM) was used to visualize the morphology of the SEI layer formed on the graphite electrode after electrolyte electroreduction.

2 Experimental section

2.1 Reagents

Glutaronitrile (GLN) (>99 %), dimethyl carbonate (DMC) (>99 %), metallic lithium, and lithium lithium bis-(trifluoromethane sulfonyl) imide (LiTFSI) salts were purchased from Aldrich and used as received without any further purification. Electrolyte solutions were prepared in a glove box filled with argon containing less than 0.5 ppm of water. Electrolytes were prepared by adding the appropriate weight of LiTFSI to GLN or GLN/DMC mixtures and the amount of residual water in electrolytes was measured using a Metrohom Karl–Fisher titrator. The water content of all prepared electrolytes was found to be below 20 ppm.

2.2 Ionic conductivities

Ionic conductivities were measured using a Crison (GLP 31) digital multi-frequency conductimeter in a thermostated cell. Ionic conductivity measurements was carried out at 20 °C and the cell constant was determined using a standard solution of $LiPF_6$ (1 M) in EC/PC/3DMC ($\sigma = 12.0$ mS cm^{-1} at 25 °C).

2.3 Viscosities' measurements

Viscosities' measurements were conducted using a TA AR1000 stress rheometer over a temperature range from 20 to 65 °C. The liquid viscosities were determined using a cone-plane geometry. Typically, the liquid sample volume is 0.5 cm^3.

2.4 Electrochemical measurement

Galvanostatic charge–discharge experiments and cyclic voltammetry were performed using a Multichannel Galvanostat-Potentiostat (MPG2-Biologic S.A) piloted by an Ec Lab V9.97 interface. Electrochemical measurements were performed using a two-electrode configuration as well as the Teflon® Swagelok® system. Graphite SLP 30 coated on a copper disk current collector (diameter: 1 cm; active mass: 4.4 mg cm^{-2}) was used as working electrode and a Li foil as counter electrode. Microporous polypropylene membrane (thickness $h = 25$ µm and pore diameter $\emptyset = 0.2 - 0.5$ µm) filled with the electrolyte solution was used as separator and the cell was assembled in a glove box filled with argon. Graphite anode and separators were dried under vacuum for at least 3 days at 80 °C before assembling electrochemical cells test. When galvanostatic charge–discharge technique was used, the potential of the working electrode was recorded with regard to the potential of the Li/Li^+. All impedance measurements (Solartron 1230) were performed at the open circuit voltage of the electrochemical cell between 1 MHz and 0.1 Hz with signal amplitude of 5 mV.

2.5 Scanning electron microcopy (SEM)

Scanning electron microcopy (SEM) was performed with Zeiss ULTRA Plus Field Emission microscope; before SEM analysis, a platinum layer (few nm) was deposited by the sputtering technique on the graphite disk electrode in order to avoid any charging effect on the insulating SEI layer.

2.6 Contact angle measurements (CA)

Contact angle measurements (CA) were measured using the sessile drop method and G-11 goniometer (Krüss, Germany) at room temperature (20 ± 1 °C). 5 measurements were performed for each sample and were used to calculate the arithmetic mean and the standard deviation.

3 Results and discussion

The solubility of $LiPF_6$ and LiTFSI salts in pure GLN was compared and, as expected, the solubility of $LiPF_6$ was found to be very low compared to LiTFSI. Indeed, as reported in the work of Abu-Lebdech et al. [13], dinitrile solvents dissolve LiTFSI salt to more than 1 molar, but poorly dissolve $LiPF_6$. So, LiTFSI was chosen as lithium salt instead of LiPF6 for the preparation of all electrolytes in this study.

GLN is polar and exhibits a high dielectric constant ($\varepsilon = 37$) which allows a good ionic dissociation of salts. In addition, GLN has a good thermal stability with a low melting point (−29 °C), a very high ebullition point (285 °C), and a moderate viscosity which still remains higher than the currently used alkyl carbonates. In Table 1, the main properties of GLN are displayed and, for comparison, some common solvents used in electrochemical storage systems.

In order to lower the viscosity of GLN and thus increase the ionic conductivity, DMC was used as co-solvent since it possesses a low viscosity and a good miscibility with GLN. The graph reported in Fig. 1 shows the evolution of the ionic conductivity of LiTFSI in GLN/DMC binary mixtures at 25 °C.

As shown in Fig. 1, and as expected from the viscosities of the pure solvents, the conductivity increases sharply when DMC is added to GLN. The conductivity reaches a maximum of 5.8 mS cm^{-1} at a mass fraction of DMC of 0.6. At a higher mass fraction of DMC, the conductivity decreases, probably due to the formation of non-conducting ion pairs in mixtures of lower permittivity, i.e., mixtures with high amount of DMC. The activation energies were determined for GLN/DMC (1:1(wt%), (1:3(wt%)), and (1:0) mixtures containing LiTFSI salt using the Arrhenius equation (Eq. 1) and plotting ln (σ) versus $1/T$ (Fig. 2).

$$\sigma = \sigma_0 \exp\left(\frac{-E_{a,\sigma}}{\mathrm{RT}}\right) \quad (1)$$

Table 1 Physico-chemical data of GLN and common solvents used in electrochemical storage systems

Solvent	Abr	MW	Dielectric (ε)	Density (d)	m.p (°C)	b.p (°C)	Viscosity η (mPa s)
Ethylene carbonate [22]	EC	88	89 (40 °C)	1.321	39	248	1.9 (40 °C)
Propylene carbonate [22]	PC	102	64.9	1.200	−49	242	2.53
Dimethyl carbonate [22]	DMC	90	3.1	1.063	3	90	0.59
Diethyle carbonate [22]	DEC	118	2.8	1.065	−43	127	0.75
Ethyl methyl carbonate [22]	EMC	104	2.9	1.006	−55	110	0.65
Acetonitrile [23]	ACN	53	35.9	0.800	−49	82	0.35
Glutaronitrile [23]	GLN	94	37.0	0.995	−29	285	4.79
Vinylene carbonate [22–24]	VC	86	41	1.355	22	162	–
γ-buturolactone [22]	GBL	86	42	1.100	−44	204	1.70

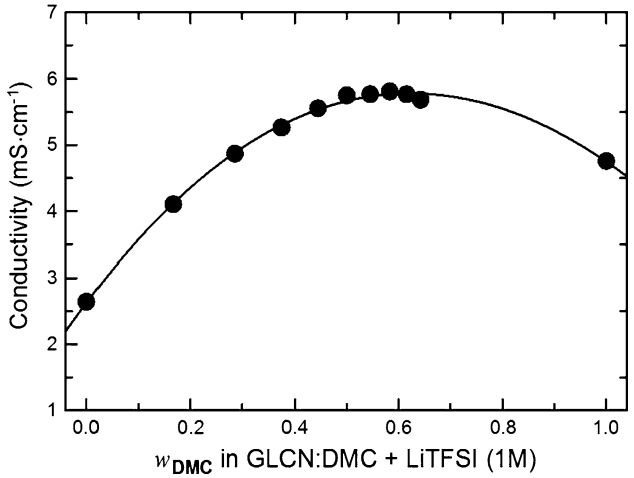

Fig. 1 Evolution of conductivity of GLN/DMC mixtures containing LiTFSI (1 M) as a function of DMC mass fraction (w_{DMC}) at 25 °C

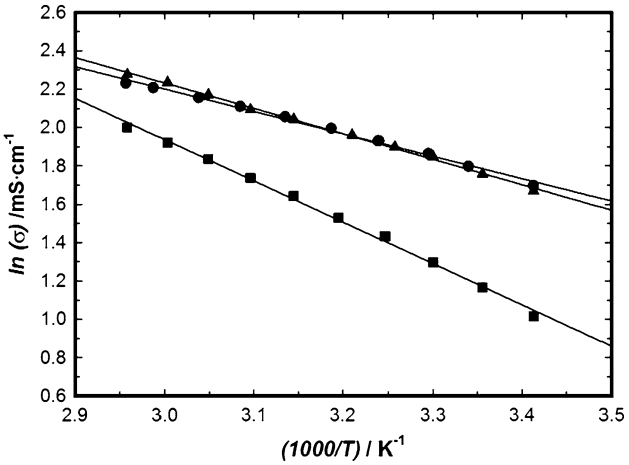

Fig. 2 Arrhenius plots of the conductivity of pure GLN and in mixture with DMC containing LiTFSI (1 M), *square* GLN/3DMC, *circle* GLN/DMC, *triangle* GLN

in the Eq. 1, σ_0 denotes the pre-exponential constant, T is the temperature, $E_{a,\sigma}$ is the activation energy, and R is the gas constant. At a given composition, the Arrhenius plots are linear and $E_{a,\sigma}$ could be deduced from the slope of the correlation (Fig. 2). $E_{a,\sigma}$ is a thermodynamic parameter which reflects the sensitivity of the electrolyte conductivity to temperature variations. Results indicate that the activation energy is lowered when DMC is added to the pure GLN (1 M, LiTFSI) electrolyte. Indeed, $E_{a,\sigma}$ was found to be 14.7 and 9.7 J mol^{-1} for GLN/DMC (wt%)- and GLN/3DMC (wt%)-based electrolytes, respectively, while it reaches 17.90 J mol^{-1} for pure GLN-based electrolyte.

The addition of solvent with low viscosity (DMC) could decrease the Van der Waals attractive forces between GLN molecules, and thus decrease the viscosity and the activation energy of the mixtures. It can also be concluded from the Fig. 2 that the conductivity is quite similar for the two compositions (for GLN/DMC and GLN/3DMC) on the all ranges of considered temperature.

Viscosity studies provide a useful understanding on the mobility of ions in liquid electrolytes. Figure 3 shows the evolution of the viscosity of the electrolytes with temperature. As expected, the viscosity decreases when increasing temperature for all the compositions. However, this behavior is more pronounced for pure GLN-based electrolyte when compared to GLN/DMC mixtures. The activation energies for the viscosity are determined in the same way as for the conductivity, using an Arrhenius plot (ln(η) vs. 1/T):

$$\eta = \eta_0 \exp\left(\frac{-E_{a,\eta}}{\mathrm{RT}}\right) \quad (2)$$

In Eq. 1, η_0 denotes a pre-exponential constant and $E_{a,\eta}$ the energy of activation for the viscosity.

As predicted from the Walden's rule, viscosities and conductivities are linked quantities. This rule was deduced from the empirical observation that the product $\sigma . \eta$ remains approximately constant when the viscosity is changed at fixed temperature. Walden's rule can be used to investigate how σ is correlated to η. When ions move through the solvent under an electrical field E, they undergo two opposed forces, an electrical force, zeE, and a frictional opposite force, $F_{fri} = 6\pi\eta r\mu$, where z, e, r, and μ are the valence, the elementary charge (1.602×10^{-19} °C), the hydrodynamic radius, and the electrical mobility of the ion, respectively. The two forces act in opposite directions and thus, the accelerating effect of the electrical force is balanced by the friction force resulting from the viscosity of the medium:

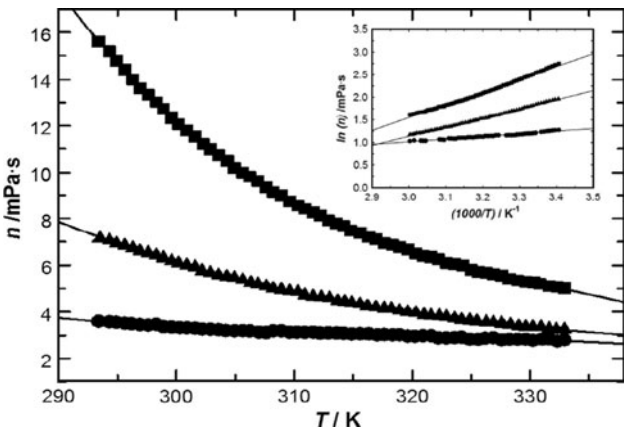

Fig. 3 Evolution of the viscosity of GLN/LiTFSI-based electrolytes with temperature, *circle* GLN/3DMC, *triangle* GLN/DMC, *square* GLN. In *inset*, the corresponding Arrhenius plots

Table 2 Conductivity, viscosity, and Walden's product at 25 °C

Electrolytes containing LiTFSI (1 M)	Conductivity (mS/cm)	Viscosity (mPa s)	Walden product (W)
GLN	3.2	13.0	41.6
GLN/DMC	5.7	6.4	36.5
GLN/3DMC	6.2	3.5	22.0
DMC	4.5	1.6	7.2

$$zeE = 6\pi\eta r\mu \tag{3}$$

Keeping in mind that $\sigma \propto \mu$, Eq. 3 leads to Walden's rule, inasmuch as the hydrodynamic radius can be considered as constant:

$$\sigma \cdot \eta = W = \text{cte} \tag{4}$$

The change of W with the composition of the mixture indicates that the decrease of the viscosity was not fully counterbalanced by the increase of the ionic conductivity. Thus, ions' pairing and solvation effects inside the electrolyte cannot be neglected [25]. In addition, low values of the Walden product may indicate a lower salt dissociation and a higher ion pairing inside the electrolyte solution. Data reported in Table 2 show that W decreases when the amount of DMC increases, meaning that either the dissociation of the Li salt decreases or the hydrodynamic radius of the ions (essentially Li^+) is changed owing to solvation effects. Indeed, the solvation of ions in the electrolyte is strongly linked to the composition of the solvent mixture and we believe that Li ion is specifically solvated by GLN molecules which possess relatively high donor ability, i.e., higher strength of solvation of cations compared to DMC [26]. On the other hand, specific interaction between GLN and Li^+ implies that such increase of GLN in the mixture would increase the ionic conductivity as it was previously reported by H. Nakamura et al. for PC/DMC mixtures, even the increase of the viscosity when PC was added [27].

In the present work, the conductivity reaches a plateau and then it decreases (Fig. 2), indicating that the specific interaction between GLN and lithium ions may be partially inhibited by the high viscosity of GLN. When the mass fraction of DMC increased, even if the viscosity decreased, the formation of more ion pairs in the electrolytes (low Walden product) could limit the ionic conductivity. In fact, GLN/3DMC appears to be more appropriate to the formation of ions pair (low Walden product) as a consequence of the decrease of dielectric constant of the solvent when a high amount of DMC (low dielectric constant) was added. Therefore, such an increase of ionic conductivity (and thus Li^+ transport) in our case could be attributed to the decrease of the viscosity of the electrolyte.

The electrochemical behavior of the graphite electrode in GLN/DMC mixed electrolytes was evaluated in a half cell configuration using cyclic voltammetry. Figure 4a, b shows the first and the second cyclic voltammograms (CV) obtained in GLN, and GLN/DMC mixtures containing LiTFSI.

As shown in Fig. 4a in the GLN/LiTFSI electrolyte, the CV curve displays a significant cathodic current starting from 1.2 V versus Li/Li^+. Three successive reductions waves starting from 1.12, 0.75, and 0.14 V versus Li/Li^+, are observed: the first reduction is attributed to direct and irreversible reduction of the electrolyte onto graphite anode to form insoluble and soluble species by the following reaction [28]:

$$Li(CF_3SO_2)_2N + 4e^- + 4Li^+ \rightarrow Li_3N + 2CF_3SO_2Li$$

The second and large reduction starting from 0.75 V may be attributed to direct reduction of dinitrile solvent on the electrode and/or a possible co-intercalation of solvated Li ions into graphite, while the small reversible peak located at about 0.05 V could be attributed to lithium intercalation–deintercalation into graphite. During the second scan, the gravimetric reduction current between 1.2 and 0.2 V drastically diminishes and the peaks located at 1.12 V

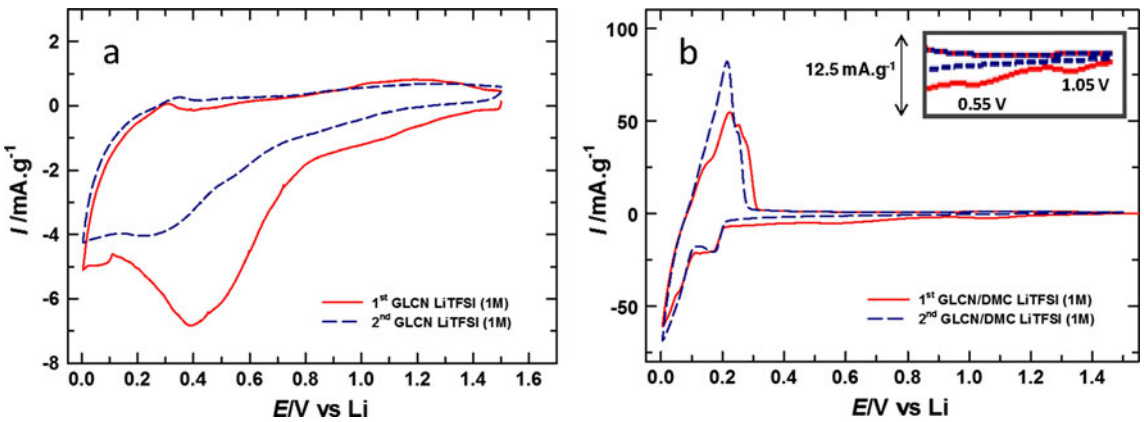

Fig. 4 First and second voltammetric scans of graphite electrode in 1 M LiTFSI with **a**-GLN, **b**-GLN/DMC ($w_{DMC} = 0.5$) at 0.05 mV s^{-1}. In the insert: potential range between 1.2 and 0.4 V

almost disappear, indicating that the electrochemical process occurring at the first voltammetric scan would be mainly due to the irreversible formation of an SEI layer. When GLN/DMC mixtures were used, the electrochemical response was very different (Fig. 4b). During the first CV cycle, an irreversible current is observed between 1.4 and 0.2 V, followed by a reversible intercalation deintercalation of lithium ion between 0.2 and 0 V. The reduction peaks observed at about 1.05 and 0.55 V versus Li/Li^+ could be considered as the same as those observed for pure GLN electrolyte.

During the second scan, all reduction peaks fully disappear, and the solvated lithium intercalation was suppressed (peak at 0.55 V vs. Li), indicating that the formation of the SEI layer is achieved. The peaks located between 0.25 and 0 V clearly indicate that lithium intercalation–deintercalation into graphite occurs reversibly [15]. This behavior is proof that the quality of the SEI layer was improved when DMC was added. A good SEI layer prevents further electrolyte decomposition and solvent co-intercalation and thus improves the kinetics and reversibility of lithium intercalation into graphite. The observed CVs in this case show some obvious similarities with those usually reported for graphite anode in more conventional electrolytes (EC/DMC or EC/PC/DMC) [25, 29]. In addition, it is worth noting that DMC can be decomposed directly onto graphite anode to form insoluble species. The main product of the decomposition of DMC is the insoluble lithium salt Li_2CO_3 as previously reported by Aurbach et al. [30]. The product of DMC decomposition could participate in the passivation of the anode and hence improve its cyclability. In GLN alone, as can be seeing in Fig. 4a, no significant reversible lithium intercalation–deintercalation is observed. The SEI layer could be less Li^+ conductive or/and the graphite anode is exfoliated by the co-intercalation of GLN molecules.

The graphite negative electrodes were examined by SEM after the CV cycling. As shown in Fig. 5 on the SEM pictures, we can easily identify the SEI layer formed on the graphite electrode after being cycled. When GLN was used as a single solvent (Fig. 5b), the SEI layer seems to be inhomogeneous, and the electrode surface is not fully covered with this layer. Figure 5d (GLN/3DMC) and Fig. 5c (GLN/DMC) show that the SEI layer is smoother and more homogeneous when DMC is used as co-solvent and that the whole surface of graphite is covered. Homogeneous and compact SEI layer should enhance the electrode cyclability by facilitating lithium ions' intercalation and preventing solvent intercalation and decomposition at the graphite anode.

On the basis of the SEM observations, the more homogeneous SEI layer formed on the graphite surface could be explained by the diminution of the viscosity of the electrolyte owing to DMC co-solvent that could improve the electrode/electrolyte interface and graphite wettability. Indeed, as discussed by our group in a recent paper [30], interfacial properties such as wettability of the materials by the electrolyte play key roles which can influence the

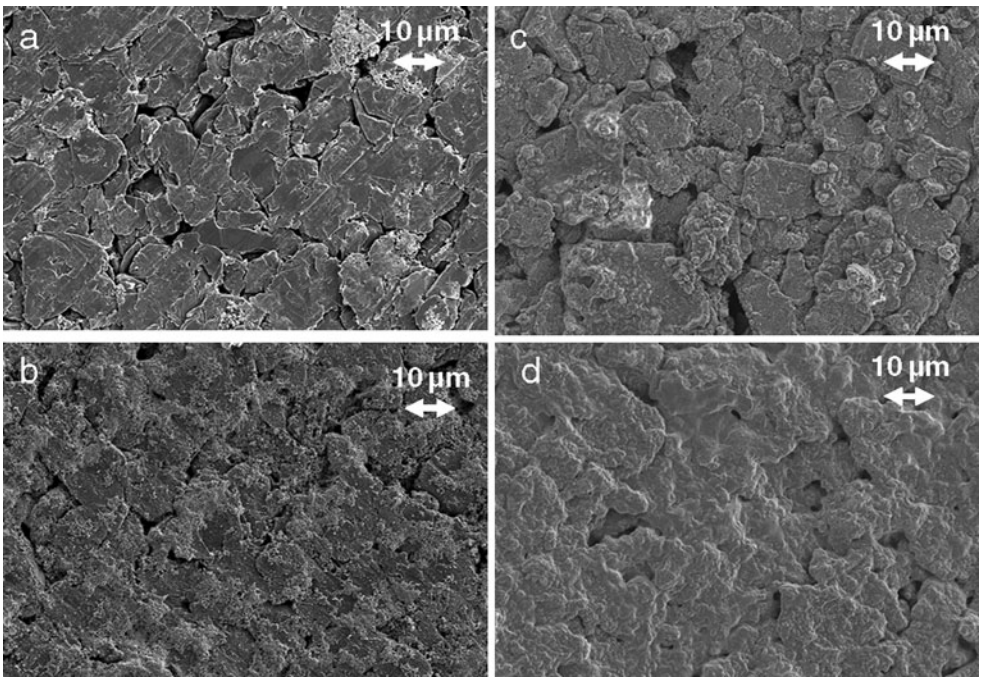

Fig. 5 SEM images of **a**-Graphite electrode, **b**-Graphite electrode after been cycled in GLN-LiTFSI 1 M, **c**-Graphite electrode after been cycled in GLN-DMC 1 M LiTFSI, **d**-Graphite electrode after been cycled in GLN-3DMC 1 M LiTFSI

performances of the electrode. Figure 6 shows the evolution of the contact angle (CA) of the graphite surface (SLP30) with the increase of the mass fraction of the DMC in the electrolyte. From those data, it is obvious that the wettability of the electrode is enhanced by adding DMC in the electrolyte. In pure GLN, the material exhibits a relatively low wettability (CA = 38°) contrasting with its very good wettability in pure DMC (CA = 7°). When mixtures of GLN/DMC (1:1 and 1:3) were used, the CA decreases drastically, indicating that the contact and the wettability of the materials were improved.

Impedance measurements were performed on the SW electrochemical cells using different GLN-based electrolytes in order to highlight the effect of DMC on the evolution of the electrode/electrolyte interface. Figure 7a, a_1, b, b_1 shows the Nyquist plot deduced from impedance measurements recorded before and after voltammetric cycling. As can be seen, the impedance spectra before and after cycling show some obvious differences. Before cycling (Fig. 7a, a_1), impedance spectra show a depressed semicircle in the region of high frequencies of the Nyquist diagram. The semicircle can be assigned to the electrode/electrolyte interface and is characterized by its characteristic frequency, i.e., frequency at the top of the semicircle. The characteristic frequency is directly linked to the chemical nature of the interface (electrode and electrolyte), and its value remains unchanged between the three electrolytes before voltammetric cycling ($f = 398.1$ Hz). The intercept of the semicircle with the X-axis is related to the conductivity of the electrolyte and its diameter corresponds to the polarization resistance of the electrode/electrolyte interface (R_p). When DMC is added, the diameter of this semicircle decreases as well as the intercept with the X-axis. This means that the ionic conductivity through the electrochemical cell increases and that R_p at the interfaces

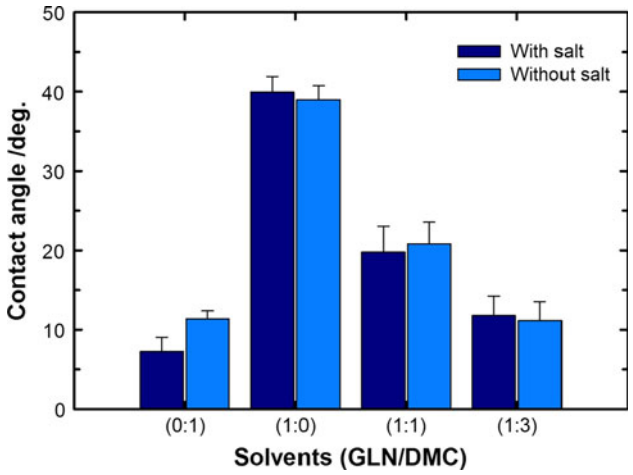

Fig. 6 Evolution of the contact angle of graphite as function of the mass fraction of DMC in GLN/DMC mixtures

decreases. The total serial resistance, which includes all contributions from the electrolyte, the separator, and the contact resistances, is deduced from the intercept of the impedance spectra with the X-axis at high frequencies the values of which are reported in Table 3. In the region of high frequencies, the impedance spectra show a Warburg-type behavior in the case of GLN. When DMC is added, the electrodes/electrolytes interface showed a marked capacitive behavior as the −Im (Z) versus Re (Z) plots follow an almost vertical line in the medium and low frequencies regions. The capacitive region is shifted to higher frequencies (Fig. 7a_1) when the amount of DMC decreases, indicating that charge accumulation with GLN/DMC is more difficult compared to GLN/3DMC electrolyte. Such observations could be explained by the less favorable diffusion of ions because of the high viscosity of the electrolyte.

After been cycled (Fig. 7b, b_1), the electrode/electrolyte interface exhibits a more depressed semicircle in the high and medium frequencies regions which can be attributed to the porous SEI layer. The characteristic frequencies of the semicircles were changed indicating that the chemical nature of the interfaces has been changed due to the formation of the SEI layer. Similar characteristic frequencies were found with GLN/DMC and GLN/3DMC ($f = 398.1$ Hz). This result could indicate that the nature of the interface is quite comparable. As the diameter of the semicircle and the total serial impedance of the cell are decreased, it is concluded that the SEI layer is enough ion conducting for Li intercalation/deintercalation into the graphite anode. The total impedance of the cell decreases in the order GLN (LiTFSI) > GLN/DMC (LiTFSI) > GLN/3DMC (LiTFSI) as shown in Fig. 7b. As shown in Table 4, R_{SEI} decreases after cycling and reaches 75 Ω for GLN/3DMC after 3 voltammetric cycles, while a value of 830 Ω was observed for GLN as single solvent. These findings could be interpreted either in terms of difference in chemical structure of the SEI (obtained with or without DMC) or in terms of a difference in its porosity and thus in terms of ionic conductivity. Furthermore, CVs show that no significant lithium intercalation was observed in pure GLN and the solvent may co-intercalate into graphite leading to its exfoliation. Impedance data of pure GLN suggest the same result since the R_{SEI} remains still too high to promote any Li ion transport (830 Ω). It is worth noting that the diminution of R_{SEI} of the electrode/electrolyte interface is more marked when the amount of DMC in the electrolyte was high (see Table 4). Also, as can be seen in the impedance spectra, in the low frequency region, the response of graphite in GLN/DMC and GLN/3DMC before cycling (Fig. 7a_1) exhibits an almost vertical line indicating a purely capacitive behavior. After being cycled (Fig. 7b), the impedance of graphite/electrolyte interfaces decreases and exhibits a "Warburg"-type behavior at medium frequencies

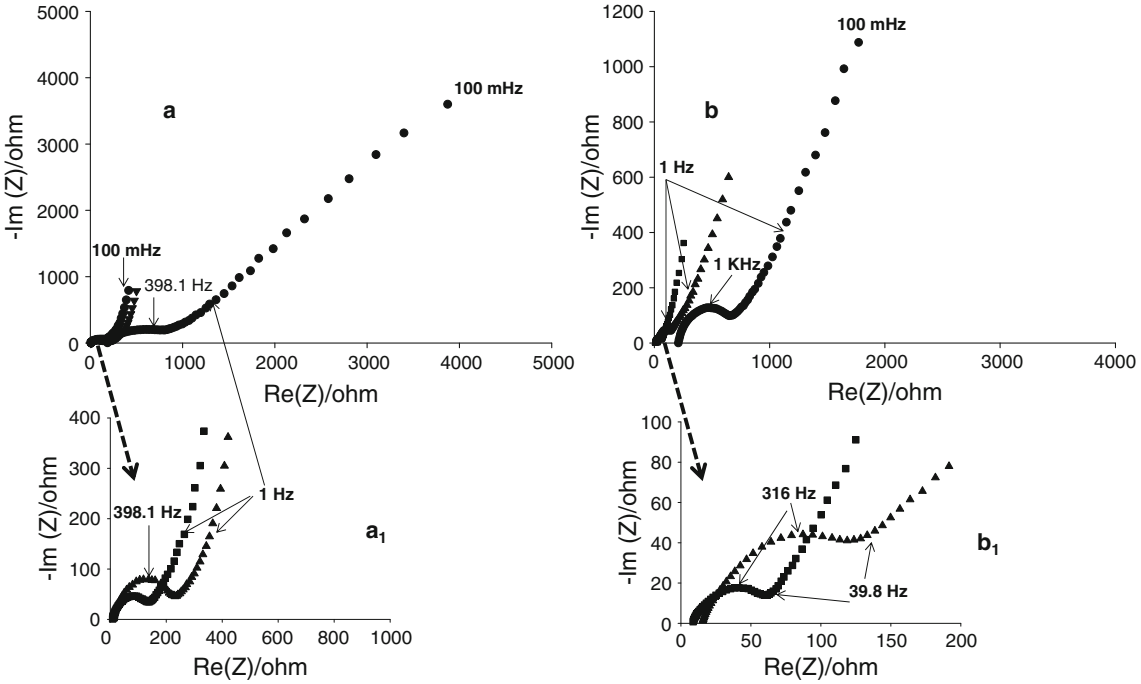

Fig. 7 Nyquist diagrams deduced from impedance measurements using different GLN- and LiTFSI-based electrolytes before and after CV at 0.05 mV s^{-1}. Before CV: **a** (**a**$_1$, *Enlarged scale*); and after CV: **b** (**b**$_1$, *Enlarged scale*). GLN (*Disk*), GLN/DMC (*triangle*), and GLN/3DMC (*square*)

Table 3 Serial (R_s) and polarization (R_p) resistances estimated from the Nyquist plot of cell impedance using different GLN-based electrolytes

Electrolyte (LiTFSI)	R_s (Ω)		R_p (Ω)	
	0 cycle	3rd cycle	0 cycle	3rd cycle
GLN	167	212	1,080	830
GLN/DMC	10	16	252	170
GLN/3DMC	7	8	162	75

(39.8 Hz in Fig. 7b$_1$) which reflect the resistance toward diffusion of ions trough the SEI. The Warburg impedance decreases when the amount of DMC was increased indicating that the SEI layer is more favorable to the conduction of ions. Such a result could be explained by higher conductivity or/and more porous SEI layer on graphite anode when DMC was used as co-solvent and more when its amount was increased in the electrolyte.

As it was reported by Shengshui Zhang et al. [25], the formation of the SEI layer occurs in two steps. The first one consists of reduction of solvent/electrolyte before the lithiation of graphite (above 0.250 V) and, at this stage, the obtained layer is insulating. The second reduction step starting from 0.25 to 0.04 V consists of an irreversible reduction of the electrolyte components occurring at the same time as lithium intercalation into graphite leading to a high conductive layer. Thus, when comparing the first CVs in Fig. 4a, b, one can note that the charge consumption has mostly occurred above 0.25 V in the case of GLN electrolyte, leading to the formation of an insulating layer which greatly limits lithium intercalation. Indeed, impedance data clearly highlight the fact that the interfacial resistance attributed to the SEI was drastically decreased after cycling, especially when DMC is used as co-solvent.

The cycling performances of graphite electrode were evaluated in SW half cells using GLN LiTFSI (1 M) electrolytes at various DMC mass fractions. The first two galvanostatic charge–discharge profiles, performed under constant current value corresponding to *C*/20, are displayed in Fig. 8. During the first charge, a large irreversible capacity is observed between 1.2 and 0.2 V for all GLN/DMC electrolytes. According to previous CV results, the irreversible capacities which are 135 and 53 Ma h g^{-1} for GLN/DMC and GLN/3DMC, respectively, correspond to the reduction of the salt/solvent system. A larger capacity loss is observed when the amount of GLN is increased. In addition, no potential plateau is observed above 0.25 V versus Li/Li^+, indicating that no significant co-intercalation of solvent molecules occurs [16], even in the case of GLN as single solvent. Indeed, co-intercalation of solvent molecules, and thus graphite exfoliation, is manifested by a potential plateau as can be seen in Fig. 6d when propylene carbonate (PC) was used instead of dintrile.

The reversible specific capacity (C_{rev}) during the first cycle is 239 and 321 mA h g^{-1} for GLN/DMC and GLN/3DMC, respectively. Using GLN as single solvent, the

Table 4 Discharge capacities and columbic efficiencies of graphite negative electrode deduced from the three first cycles in different electrolytes

Electrolytes	Discharge capacity (mA h g^{-1})			Coulombic efficiency (%)		
	1st	2nd	3rd	1st	2nd	3rd
LiTFSI-GLN/DMC 1:3	369	316	310	91	99	99
LiTFSI-GLN/DMC 1:1	374	239	199	72	98	97
LiTFSI-GLN	13	11	9	0.16	–	–

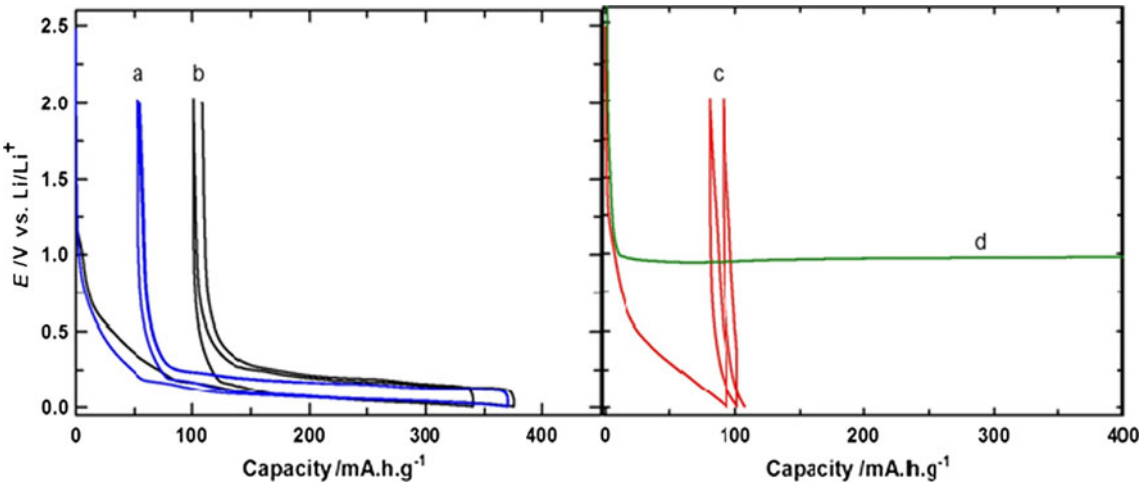

Fig. 8 Galvanostatic charge–discharge profiles of graphite electrode at *C*/20 using 1 M LiTSI in **a**-GLN/3DMC, **b**-GLN/DMC, **c**-GLN, and **d** for PC

charge–discharge profile is deeply different: A rapid and continuous potential drop starting from the OCV to 0 V is observed, while the total capacity, essentially irreversible, does not exceed 80 mA h g^{-1}. At this stage, these results clearly indicate that the use of DMC as co-solvent with GLN greatly improves the cycling capability of the graphite electrode. In Table 4, the discharge capacities and the coulombic efficiencies are reported obtained at the graphite negative electrode in electrolytes with different compositions.

The coulombic efficiencies in GLN electrolyte are very low, indicating that discharge capacity observed in the first discharge is mainly irreversible. Coulombic efficiencies increase to more than 70 % in GLN/DMC and 90 % in GLN/3DMC, indicating that charge consumption by irreversible process is decreased. Furthermore, higher coulombic efficiencies are obtained after only 2 galvanostatic charge–discharge cycles and this is proof that the lithium insertion-deinsertion into graphite occurs reversibly and that the formation of the SEI layer is rapid. The reversibility is quite good even in the case of GLN/DMC (1:1), which exhibits a relatively low value of discharge capacity (199 mA h g^{-1} after 3 cycles). This could indicate that the SEI layer is not conducting enough (or thicker: more resistive), leading to some capacity loss. In fact, as

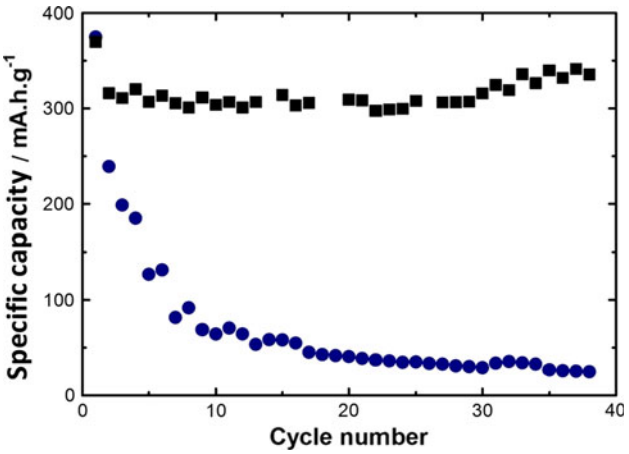

Fig. 9 Cyclability of graphite anode in GLN/DMC (*disk*) and GLN/3DMC (*square*) under constant discharge current of *C*/20 corresponding to charging current of 0.013 mA g^{-1}

discussed in the previous section (impedance experiments), the SEI layer is more conductive when GLN/3DMC was used as electrolyte solvent.

Typically, before potentials >250 mV, a certain amount of lithium ion may be utilized in the formation of the SEI film on the graphite anode and, thus, is not realizable in the subsequent delithiation. Electrolytes based on the mixtures

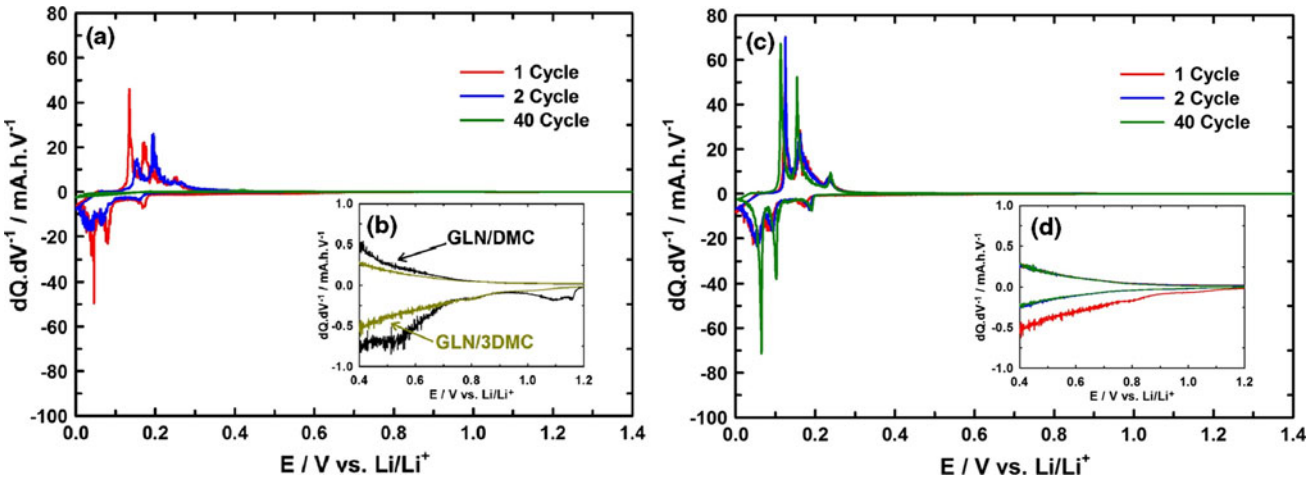

Fig. 10 dQ/dV plots, **a** and **c** 1st, 2nd, and 40th cycles in GLN/DMC and GLN/3DMC (**c**); **b** overlay of the first dQ/dV cycles of GLN/DMC and GLN/3DMC in the potential range 1.2–0.4 V (irreversible region); **d** evolution of the dQ/dV in the irreversible region (1.2–0.4 V) in GLN/3DMC

of GLN and DMC facilitate rapid film formation compared to pure GLN-based electrolyte. When the amount of DMC was increased, the potential drops more sharply to reach rapidly the first lithiation plateau, suggesting that the SEI protective layer was formed more easily and thus without significant irreversible loss of lithium ion during the formation of the SEI layer. Therefore, a high amount of DMC co-solvent in the GLN-based electrolyte should be more appropriate to avoid capacitance loss in Li-ion devices.

The cycling stability of graphite anode in GLN-based electrolyte was also studied. Figure 9 shows the evolution of discharge capacity of the graphite anode when GLN/DMC and GLN/3DMC were used as electrolyte solvent. As expected, the discharge capacity of the Li/graphite cell with GLN/3DMC exhibits good discharge stability with coulombic efficiency of 99 %, which is reached since the second galvanostatic charge discharge cycle indicating that the irreversible process usually occurring at the first discharge (SEI formation) was fully finished. In addition, the discharge capacity is stable even after more than 40 cycles at constant discharge. In contrast, the cell cycled in GLN/DMC exhibits a large and rapid capacity fading. The fast fade of capacity for GLN/DMC may be due to the growth of SEI upon cycling. The SEI is less stable than that of GLN/3DMC. In addition, the coulombic efficiency obtained with GLN/DMC even after 3 galvanostatic charge–discharge (97 %) cycles may indicate that the low capacity and its fall are due to the low conductivity of the SEI layer. Charge evolution (dQ/dV) was calculated from data of Fig. 9 and plotted versus the potential. Figure 10, shows the 1st, 2nd, and 40th dQ/dV plots for GLN/DMC and GLN/3DMC. For both electrolytes, the most charge consumption takes place between 0.3 and 0 V, so it is dedicated to the reversible graphite lithiation delithiation process. Highest dQ/dV is obtained for GLN/3DMC, indicating a more lithiated graphite in this case. Above 0.3 V, the observed dQ/dV is believed to be mainly due to an irreversible process such as SEI formation; in this region, the charge consumption is higher for GLN/DMC and it may indicate the formation of a thicker and a less conductive SEI layer in accordance with impedance data. Additionally, no evolution of the dQ/dV is observed from the 2nd to the 40th cycle when GLN/3DMC is used. Thus, the SEI layer is stable after the second discharge and protects efficiently the electrode from further electrolyte degradation.

4 Conclusion

The electrochemical compatibility of negative graphite electrode has been investigated in GLN- and GLN/DMC-based electrolytes using LiTFSI as Li salt. DMC has been chosen as co-solvent owing to its low viscosity and its compatibility with graphite electrodes. First, the composition of the GLN/DMC mixture has been optimized in terms of conductivity and viscosity. Cyclic voltammetry clearly reveals the formation of an SEI at the graphite electrode surface which can be visualized by SEM images. Impedance measurements show that the interfacial resistance, mainly due to the SEI layer, decreases when the amount of DMC in the GLN/DMC mixture is increased. Under galvanostatic charging–discharging cycles at $C/20$, the coulombic efficiencies at the third cycle reach, respectively, 97 and 99 % for GLN/DMC and GLN/3DMC solvents' mixtures with LiTFSI salt. Only the GLN/3DMC mixture provides good cycling properties and reversible lithium intercalation into graphite. In the present work, only the

compatibility of GLN-based electrolyte free from any cyclic carbonate co-solvents or additives was reported. The compatibility of the optimized electrolyte formulation (GLN/3DMC) with conventional cathodes ($LiCoO_2$, $LiFePO_4$) and the electrochemical performances in full Li-ion system should also be examined.

Acknowledgments The authors would like to thank the French program ANR-Stock E (Hipascap Project, 2009) for the financial support and Pierre-Ivan Raynal for the SEM images.

References

1. Spahr M, Goers D, Markle W, Dentzer J, Wursig A, Buqa H, Vix-Guterl C, Novak P (2010) Electrochim Acta 55:8928
2. Zheng H, Jiang K, Abe T, Ogumi Z (2006) Carbon 44:203
3. Goodenough JB, Kim Y (2010) Chem Mater 22:587
4. Ratnakumar BV, Smart MC, Surampudi S (2001) J Power Sources 97–98:137
5. Novàk P, Joho F, Imhof R, Panitz J, Haas O (1999) J Power Sources 81–82:212
6. Hee Park M, Sup Lee Y, Lee H, Han Y (2011) J Power Sources 196:5109
7. Myung S-T, Natsui H, Sun Y-K, Yashiro H (2010) J Power Sources 195:8297
8. Moumouzias G, Ritzoulis G, Siapkas D, Terzidis D (2003) J Power Sources 122:57
9. Han H-B, Zhou S-S, Zhang D-J, Feng S-W, Li L-F, Liu K, Feng W-F, Nie J, Li H, Huang X-J, Armand M, Zhou Z-B (2011) J Power Sources 196:3623–3632
10. Barlow CG (1999) Electrochem Solid State Lett 2:362
11. Aurbach D, Talyosef Y, Markovsky B, Markevich E, Zinigrad E, Asraf L, Gnanaraj JS, Kim H-J (2004) Electrochim Acta 50:247
12. An Y, Zuo P, Cheng X, Liao L, Yin G (2011) Electrochim Acta 56:4841
13. Profatilova IA, Kim S, Choi N (2009) Electrochim Acta 54:4445
14. Smart MC, Ratnakumar BV, Surampudi S, Wang Y, Zhang X, Greenbaum SG, Hightower A, Ahn CC, Fultz B (1999) J Electrochem Soc 146:3963
15. Abu-Lebdeh Y, Davidson I (2009) J. Electrochem Soc 156:A60
16. Abu-Lebdeh Y, Davidson I (2009) J Power Sources 189:576
17. Nagahama M, Hasegawa N, Okada S (2010) J. Electrochem Soc 157:748
18. Yamada Y, Takazawa Y, Miyazaki K, Abe T (2010) J Phys Chem C 114:11680
19. Ue M, Ido K, Mori SS (1994) J. Electrochem Soc 141:2989
20. Ue M, Takeda M, Takehara M, Mori S (1997) J Electrochem Soc 144:2684
21. Gmitter AJ, Plittz I, Amatucci GG (2012) J Electrochem Soc 159:A370
22. Linden D, Reddy TB (2002) Handbook of batteries. McGraw-Hill, New York
23. Schwarz M, Nelson E (1970) J Chem Eng Data 15:341
24. Cossi M, Rega N, Scalmani G, Barone V (2003) V. J. Comput Chem 24:669
25. Dahbi M, Ghamouss F, Tran-Van F, Lemordant D, Anouti M (2011) J Power Sources 196:9743
26. Abe K, Hattori T, Matsumori Y (2004) US 2004/0013946 A1
27. Nakamura H, Komatsu H, Yoshio M (1996) J Power Sources 62:219
28. Laik B, Gessier F, Mercier F, Trocellier P, Chausse A, Messina R (1999) Electrochim Acta 44:1667
29. Aurbach D, Markovsky B, Weissman I, Levi E, Ein-Eli Y (1999) Electrochim Acta 45:67
30. Dahbi M, Violleau D, Ghamouss F, Jacquemin J, Van Tran F, Lemordant D, Anouti M (2012) Ind Eng Chem Res 51:5240
31. Borodin O, Smith GD (2006) J Phys Chem B 110:4971